Article

Simultaneous Enhancement of Contrast and Power of Femtosecond Laser Pulses by Nonlinear Interferometer

Yasser Nada [1,*] **and Efim Khazanov** [2]

1   Physics Department, Faculty of Science, Menofia University, Shibin El-Kom, Menofia 32511, Egypt
2   Institute of Applied Physics, Russian Academy of Sciences, Nizhny Novgorod 603950, Russia;
    efimkhazanov@gmail.com
*   Correspondence: yasersci@hotmail.com

Abstract: We showed that the nonlinear Mach–Zehnder interferometer may be used not only for enhancing temporal contrast, as proposed earlier, but also for increasing pulse power due to efficient pulse compression. The interferometer introduces into the output pulse a nonlinear phase equal to $\pi/2$. This allows increasing laser power by a factor of 1.5 only by means of a chirped mirror. Use of an additional nonlinear plate leads to a multi-fold power increase retaining the contrast enhancement.

Keywords: nonlinear Mach–Zehnder interferometer; post compression; femtosecond laser pulse contrast; self phase modulation

1. Introduction

High temporal contrast has an important role in experiments on studying the behavior of matter in extreme light fields. Temporal contrast is the ratio of the intensity at the peak of the pulse to the intensity on its pedestal. The pedestal appears, as a rule, due to amplified spontaneous emission in laser amplifiers of CPA lasers (chirped pulse amplification) [1], or due to amplified parametric emission in OPCPA lasers (optical parametric chirped pulse amplification) [2]. The most popular techniques for contrast enhancement are plasma mirrors [3], harmonic generation [4], and cross-polarized wave (XPW) generation [5]. XPW is based on cubic nonlinearity. Recently, several new ideas have been proposed for contrast enhancement, by means of a nonlinear phase induced by cubic nonlinearity: spectral filtering [6,7], spatial filtering [8], a nonlinear polarization interferometer [9], as well as a nonlinear Mach–Zehnder interferometer with symmetric arms [10]. In the latter case, the phase difference without non-linearity $\Delta\varphi_L$ equals π, and the radiation of the pedestal does not pass to the dark port (see Figure 1a). On the contrary, the main pulse acquires a nonlinear phase B (B-integral) in one channel, and a zero nonlinear phase in another one. If B is nonzero, then the dark port does not become completely dark. If $\Delta B = \pi$, then the dark port becomes a light port, and the major part of the main pulse comes through this port. As a result, the contrast will be infinitely high if $\Delta\varphi = \pi$. In practice, the contrast enhancement is determined by the inaccuracy of meeting the condition $\Delta\varphi = \pi$.

Due to self-phase modulation (SPM) in a nonlinear medium, and subsequent reflection from the chirped mirror (CM), the pulse may be compressed, and hence the peak power increases. The method is called TFC (thin film compression) [11], CafCA (compression after compressor approach) [12], or post-compression [13]. For pulses with energy of tens of Joules [14–16], the multiple compression of femtosecond laser pulses was demonstrated with almost no energy loss; for more details, see the review [17].

In this paper, we show that a nonlinear Mach–Zehnder interferometer may be used not only for contrast enhancement, but also for multi-fold pulse compression simultaneously.
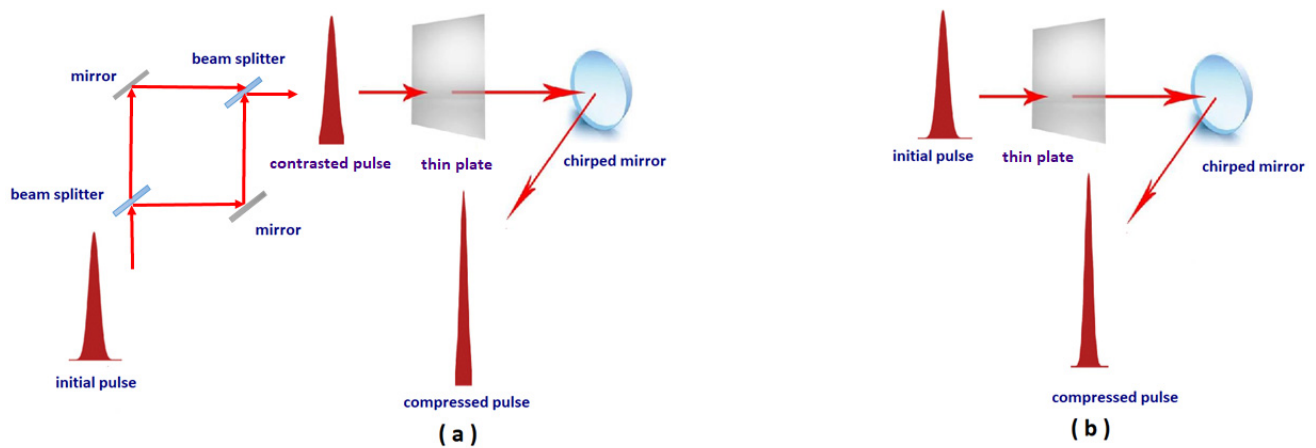
Figure 1. Optical schemes with nonlinear Mach–Zehnder interferometer (**a**) and without interferometer (**b**).

2. Nonlinear Mach–Zehnder Interferometer for Enhancement of Contrast and Pulse Compression

For the Mach–Zehnder interferometer (see Figure 1a), the expressions for intensities I_1 and I_2 at the outputs of the arms (ports) have the form [10]

$$I_1(t) = \{1 - 2(1 - R)R + 2(1 - R)R \; \cos[\Delta\varphi + 2(1 - R)B(t)]\}I_o(t). \tag{1}$$

$$I_2(t) = \{2(1 - R)R + 2(1 - R)R \; \cos[\Delta\varphi + 2(1 - R)B(t)]\}I_o(t). \tag{2}$$

Here, I_0 is the intensity at the interferometer input ($I_0 = I_1 + I_2$); $\Delta\varphi$ is the linear phase difference acquired by the pulses during propagation along the interferometer arms; $B(t) = (2\pi/\lambda)I_o(t)n_2 L$ is the nonlinear phase (B-integral) accumulated in both beam splitters; L is length of the beam path in the beam splitters; λ is the wavelength; n_2 is the nonlinear refractive index; and R is the reflectivity of the beam splitters.

Under the conditions $\Delta\varphi = \pi$ and R = 0.5, the value of I_1 in Equation (1) may be exactly zero in the absence of a nonlinear phase (B = 0). On the other hand, at high intensity, the nonlinear phase is accumulated, and the intensity I_1 takes on a maximal value, provided that B = π, $\Delta\varphi = \pi$ and R = 0.5. As a result, the pulse emerging at this port has a higher contrast. Moreover, the pulse duration shortened after reflection from the CM. For example, an input pulse of 50 fs may be shortened to 38 fs [10], which is a tiny compression factor.

The first way to increase the compression factor is to use a CM to remove the chirp from the pulse. It is easy to show that the output pulse I_1 accumulates a nonlinear phase $B_{out} = \pi/2$ because output pulse accumulates nonlinear phase $B_{out} = (B1 + B2)/2$. Where, B1 and B2 is nonlinear phases in the interferometer arms 1 and 2, respectively. Since B1 = π and B2 = 0, therefore $B_{out} = \pi/2$. As shown below, this acquired nonlinear phase leads to compression to about 25 fs, which is still a modest value, because of a small value of B_{out}. The second way is to introduce an additional nonlinear phase B_{add} by adding an additional nonlinear plate before the CM (see Figure 1a). Thus, the total value of the B-integral is $B_\Sigma = \pi/2 + B_{add}$. We will study the efficiency of pulse compression in this case. As a reference, we will use compression without interferometer (without contrast enhancement) with the B-integral equal to B_Σ (Figure 1b). The reference case is obviously more robust and practical, but it does not provide any impact on the pedestal.

Contrast enhancement is purely linear physics, but pulse compression is nonlinear, so numerical calculation is needed. We performed a detailed numerical study and comparison of compression efficiency with (Figure 1a) and without (Figure 1b) interferometer.

3. Numerical Model

Pulse propagation in a nonlinear plate is described by the nonlinear Schrödinger Equation (3) [18]

$$i\frac{\partial A}{\partial \ddagger} - \alpha\frac{\partial^2 A}{\partial \tau^2} + \beta|A|^2 A + i\gamma\frac{\partial}{\partial \tau}\left(|A|^2 A\right) = 0 \tag{3}$$

where A is the normalized amplitude of the E-field, τ is the normalized time, and the coefficients α, β and γ are defined as

$$\alpha = \frac{1}{2}\frac{\partial^2 k}{\partial \omega^2}(\omega_0), \ \ \beta = \frac{n_2\,\omega_0}{c}, \ \gamma = \frac{2n_2}{c}$$

where ω_0 is the central frequency of the pulse.

We used Equation (3) for the numerical modeling of pulse propagation, both in the interferometer's beam splitters, and in thin plates. Equation (3) is solved numerically by the split step Fourier method (SSFM). This method is widely used for solving the problem of pulse propagation in a nonlinear dispersive medium. The main advantage of this method is the use of the fast Fourier transform (FFT) algorithm, which makes it faster than the finite difference methods. Therefore, we have developed a MATLAB algorithm to implement the numerical FFT algorithm. To demonstrate the compression of the pulse as a function of B_Σ, we scanned the thickness of the nonlinear media, keeping the other parameters constant: input intensity 1 TW/cm^2, input pulse duration (FWHM) 50 fs and 30 fs, and wavelength 910 nm. We chose material parameters of fused silica as the most popular material: nonlinear refractive index $n_2 = 2.75 \times 10^{-16}$ cm^2/W and group velocity dispersion $\alpha = 280$ fs^2/cm.

SPM leads to spectral broadening; the pulse becomes positively chirped. Thus, the pulse may be compressed by reflection on the CM with negative dispersion (Figure 1). We restrict the consideration to the case in which the CM introduced a purely quadratic spectral phase, i.e., group velocity dispersion only. Such a type of CMs cannot compress the pulse to a Fourier transform limit, but they are usually commercially available. In this case, the CM is embedded in the model using Equation (4)

$$A_{compressed}(t) = \mathbf{F}\left[e^{\frac{-i\alpha(\omega-\omega_0)^2}{2}}\,\mathbf{F}^{-1}\left(A_{chirped}(t,z)\right)\right] \tag{4}$$

where $A_{compressed}$ is the amplitude after compression (after reflection from the CM) and $A_{chirped}$ is the amplitude of the field incident on the CM, $\mathbf{F}$ and $\mathbf{F}^{-1}$ are the direct and inverse Fourier transforms, respectively. The parameter α is the group velocity dispersion parameter of the CM.

Using Equations (3) and (4), we found the output pulses both for the setup with (Figure 1a) and without interferometer (Figure 1b).

4. Results and Discussion

The primary effect of SPM is spectral broadening. So, first of all, we compare the spectral bandwidth before the CM. Then, we should choose the CM dispersion α_{opt}. It may be chosen to minimize the compressed pulse duration or to maximize peak power. However, we prefer the last case, because increasing the pulse power is a primary goal for most applications. Furthermore, we study pulse shortening and power enhancement.

4.1. Spectral Broadening

The results of calculations are shown in Figure 2. The pulse in the scheme with interferometer has a wider spectral bandwidth than that without interferometer, even though B_Σ is the same. This phenomenon is explained as follows. At the interferometer output (Figure 1a), the beam is a sum of two beams: one with B = 0 and the other with B = π. The spectrum of the first beam is not broadened at all, while the spectrum of the second one is broadened much stronger than the spectrum of the single beam with $B_\Sigma = \pi/2$ in the reference case (Figure 1b). In other words, due to the nonlinear nature of SPM, the spectral broadening with interferometer is higher than in the case without the interferometer, even if $B_\Sigma = \pi/2$ in both cases (see Figure 2a,c). An additional nonlinear plate increases B_Σ up to 5, but keeps this difference (Figure 2b,d).
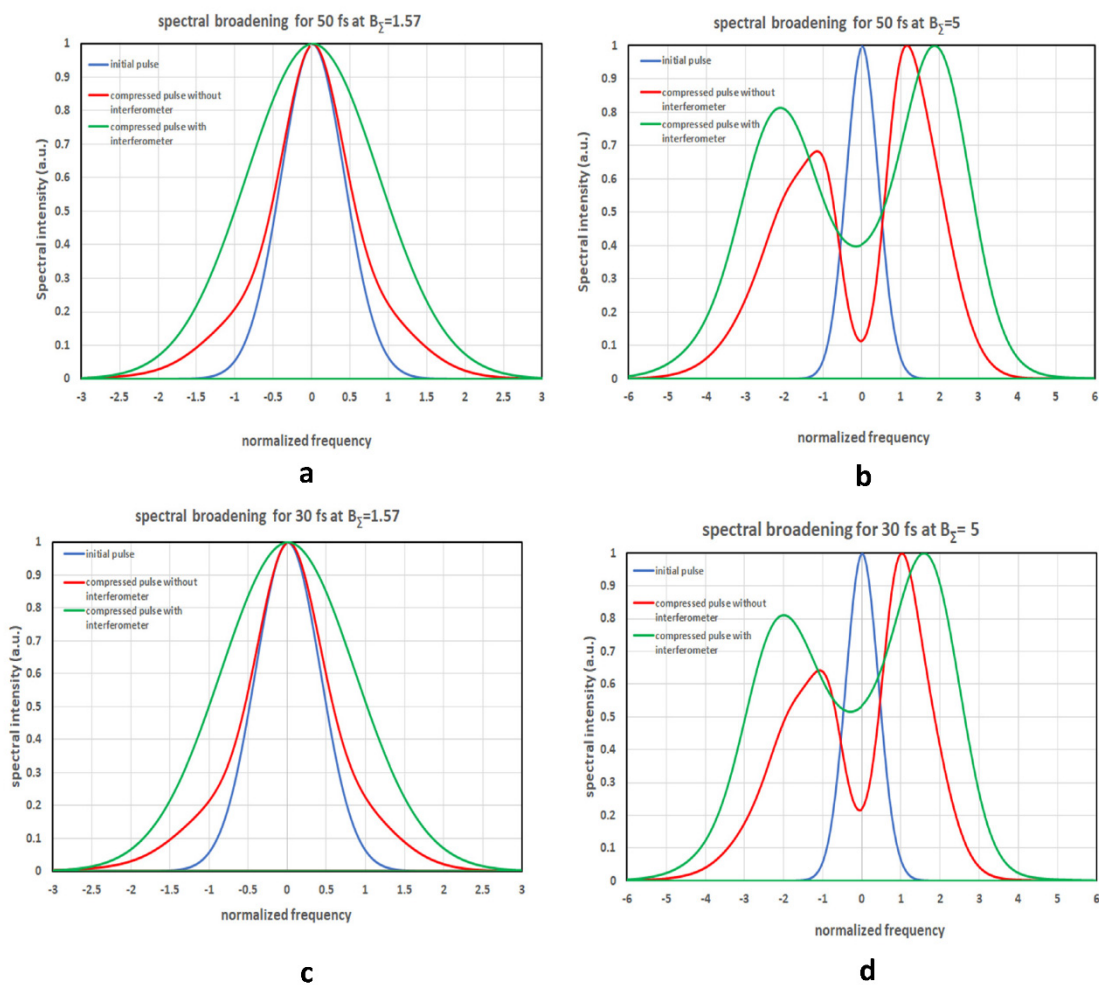
Figure 2. Spectrum of the initial pulse, compressed pulse in the scheme with interferometer (Figure 1a), and compressed pulse in the scheme without interferometer (Figure 1b) for 50 fs (**a,b**) and 30 fs (**c,d**) input pulses at $B_\Sigma = \pi/2$ (**a,c**) and $B_\Sigma = 5$ (**b,d**). Horizontal axes are normalized to the input pulse bandwidth.

The spectra for 50 fs and 30 fs input pulses are very similar (note that the horizontal axes are normalized to the input pulse bandwidths 8.82×10^{12} Hz and 1.47×10^{13} Hz for 50 fs and 30 fs, respectively). The small difference between 50 fs and 30 fs at $B_\Sigma = 5$ is due to the fact that the bandwidth for 30 fs input pulse becomes comparable to the optical frequency.

4.2. Optimal Chirped Mirror Dispersion α_{opt}

As mentioned above, we defined the optimal CM dispersion α_{opt} as a dispersion which maximizes compressed pulse peak power. When CM dispersion is not exactly equal to α_{opt}, the compressed pulse power is smaller. We calculated α_{opt} as a function of B_Σ. The results are shown in Figure 3, from which it is seen that correcting the quadratic spectral phase component for higher values of the B-integral necessitates a lower (in modulus) chirped mirror dispersion α_{opt}. Moreover, it is clear from Figure 3 that α_{opt} is smaller in the case with interferometer than without it. The smaller value of α_{opt} provides a practical advantage, because the fabrication of CM with a higher dispersion is a more serious challenge. It is worth noticing that, at a high value of B-integral, α_{opt} is almost independent of B_Σ. Hence, the same CM may be used for a B-integral in a wide range of values, eliminating the impact of instability of the laser parameters.

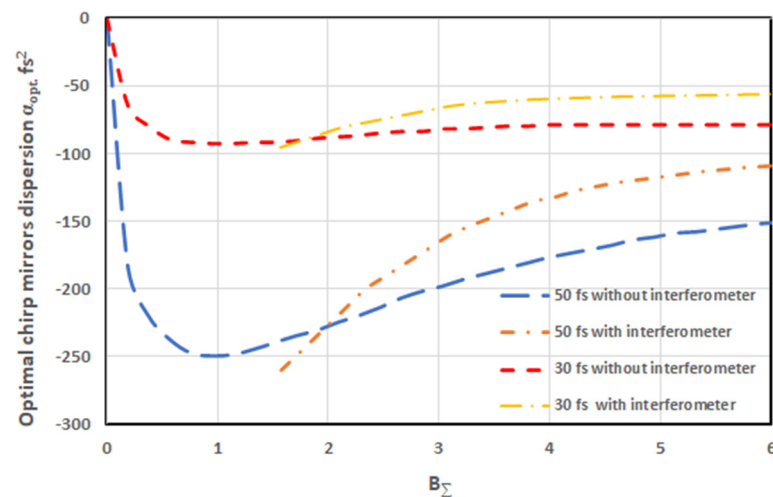**Figure 3.** B_Σ-dependence of parameter α_{opt} for different pulse durations with and without interferometer.

4.3. Pulse Compression

The results are shown in Figure 4. The compressed pulse in the scheme with interferometer is even shorter than in the scheme without interferometer. It is explained by the wider spectrum (see Figure 2). For instance, at $B_\Sigma = 5$, for 50 fs input pulse, the compressed pulse duration decreased to about 14 fs in the scheme without interferometer, and to about 12 fs with interferometer; for the 30 fs input pulse, the compressed pulse duration decreased to about 9 fs in the case without interferometer, and to about 7 fs in the scheme with interferometer.

In addition, the intensity in the compressed pulse wings is lower in the case with interferometer because the interferometer remains closed for the input pulse tails, and the chirp in the tails differs greatly from the linear chirp. So, removing the tails from the input pulse causes the compressed pulse to be closer to the Fourier transform limited one (cf. the green and red curves in Figure 4). Thus, from the pulse compression viewpoint, the case with interferometer (Figure 1a) is more preferable than the reference case (Figure 1b).

4.4. Peak Power Increase

From the viewpoint of peak power, the case with interferometer (Figure 1a) strongly differs from the reference case (Figure 1b). The latter is energy lossless, while the first one is not. Energy is lost because the dark port of the interferometer becomes perfectly light only at $B = \pi$, i.e., only at $t = 0$, i.e., for the central part of the pulse. For $t \neq 0$, the interferometer transmission is below 100% by virtue of $B \neq \pi$. For the pulse periphery, $B \ll \pi$ and the pulse do not pass through the interferometer at all. The energy transmission of the interferometer for a Gaussian pulse with $B\,(t = 0) = \pi$ is 76% for any pulse duration. This inevitable disadvantage reduces the power of compressed pulses. Nevertheless, as seen from Figure 4, the peak power is almost the same for both cases. Figure 5 shows that this is true for any value of B-integral. In spite of 24% energy loss in the interferometer, the superiority of the case without interferometer is below 10%. This is explained by more efficient pulse compression in the case with the interferometer.
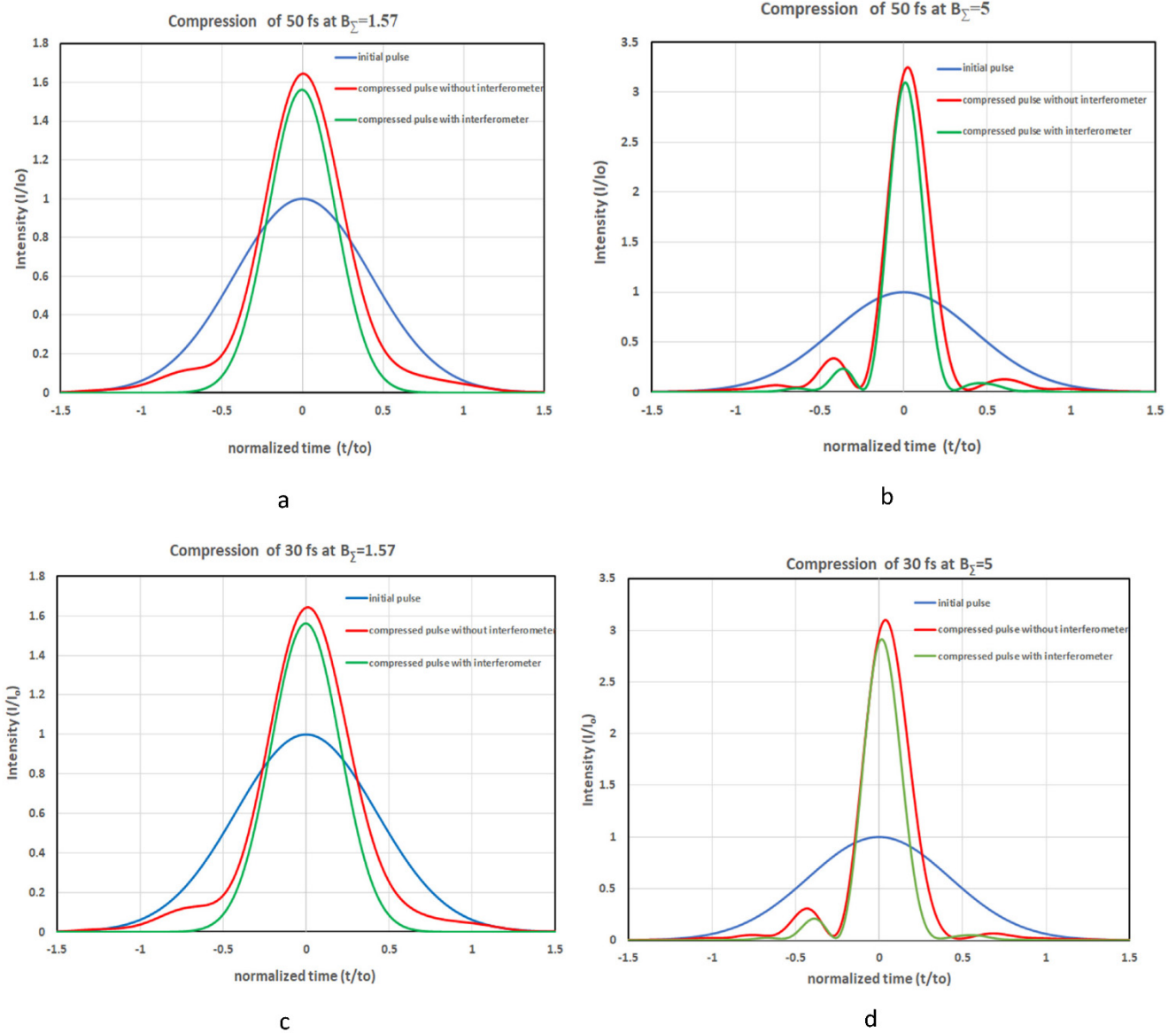
Figure 4. Shapes of the initial pulse, compressed pulse in the scheme with interferometer (Figure 1a) and compressed pulse in the scheme without interferometer (Figure 1b) for 50 fs (**a,b**) and 30 fs (**c,d**) input pulses at $B_\Sigma = \pi/2$ (**a,c**) and $B_\Sigma = 5$ (**b,d**).
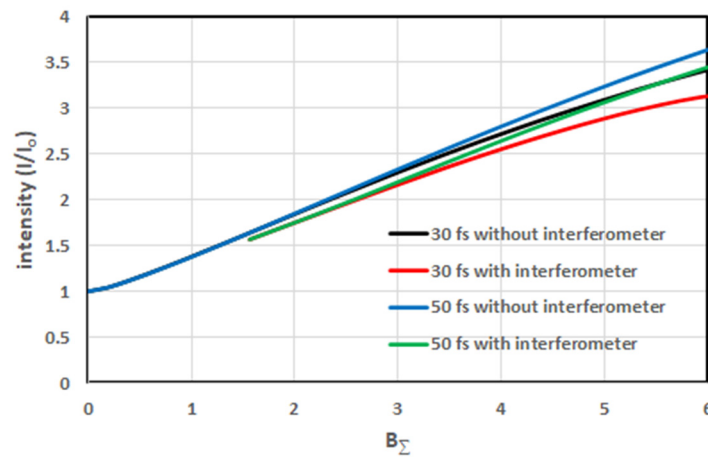

Figure 5. Output pulse intensity as a function of B- integral.

5. Conclusions

Numerical modeling confirmed that the nonlinear Mach–Zehnder interferometer may be used not only to enhance the temporal contrast, but also to increase the pulse power due to efficient pulse compression. The pulse shortens due to self-phase modulation and a chirped mirror. Self-phase modulation occurs during propagation, both in the interferometer beam splitters, and in an additional nonlinear plate. We showed that pulse compression in the scheme with interferometer is either the same or even better than the standard compression in the scheme without interferometer and without contrast improvement.

Author Contributions: Conceptualization, E.K.; methodology, Y.N.; software, Y.N.; validation, E.K. and Y.N.; formal analysis E.K.; investigation, Y.N.; resources, Y.N.; data curation, Y.N.; writing—original draft preparation, E.K. and Y.N.; writing—review and editing, E.K. and Y.N.; visualization, E.K.; supervision E.K.; project administration, E.K.; funding acquisition, E.K.; All authors have read and agreed to the published version of the manuscript.

Institutional Review Board Statement: Not applicable.

Informed Consent Statement: Not applicable.

Data Availability Statement: Not applicable.

Conflicts of Interest: The authors declare no conflict of interest.

References

1.　Strickland, D.; Mourou, G. Compression of amplified chirped optical pulses. *Opt. Commun.* **1985**, *56*, 219–221. [CrossRef]
2.　Dubietis, A.; Jonusauskas, G.; Piskarskas, A. Powerful femtosecond pulse generation by chirped and stretched pulse parametric amplification in BBO crystal. *Opt. Commun.* **1992**, *88*, 437–440. [CrossRef]
3.　Lévy, A.; Ceccotti, T.; D'Oliveira, P.; Réau, F.; Perdrix, M.; Quéré, F.; Monot, P.; Bougeard, M.; Lagadec, H.; Martin, P.; et al. Double plasma mirror for ultrahigh temporal contrast ultraintense laser pulses. *Opt. Lett.* **2007**, *32*, 310–312. [CrossRef] [PubMed]
4.　Mironov, S.Y.; Lozhkarev, V.V.; Ginzburg, V.N.; Khazanov, E.A. High-efficiency second-harmonic generation of superintense ultrashort laser pulses. *Appl. Opt.* **2009**, *48*, 2051–2057. [CrossRef] [PubMed]
5.　Jullien, A.; Albert, O.; Burgy, F.; Hamoniaux, G.; Rousseau, J.-P.; Chambaret, J.-P.; Augé-Rochereau, F.; Chériaux, G.; Etchepare, J.; Minkovski, N.; et al. 10ˆ-10 temporal contrast for femtosecond ultraintense lasers by cross-polarized wave generation. *Opt. Lett.* **2005**, *30*, 920–922. [CrossRef] [PubMed]
6.　Buldt, J.; Müller, M.; Klas, R.; Eidam, T.; Limpert, J.; Tünnermann, A. Temporal contrast enhancement of energetic laser pulses by filtered self-phase-modulation-broadened spectra. *Opt. Lett.* **2017**, *42*, 3761–3764. [CrossRef] [PubMed]
7.　Mironov, S.Y.; Starodubtsev, M.V.; Khazanov, E.A. Temporal contrast enhancement and compression of output pulses of ultra-high power lasers. *Opt. Lett.* **2021**, *46*, 1620–1623. [CrossRef] [PubMed]
8.　Khazanov, E.A. Enhancing the time contrast and power of femtosecond laser pulses by an optical wedge with cubic nonlinearity. *Quantum Electron.* **2021**, *51*, 433–436. [CrossRef]
9.　Khazanov, E. Nonlinear polarization interferometer for enhancement of laser pulse contrast and power. *Opt. Express* **2021**, *29*, 17277–17285. [CrossRef] [PubMed]
10.　Khazanov, E.A.; Mironov, S.Y. Nonlinear interferometer for increasing the contrast ratio of intense laser pulses. *Quantum Electron.* **2019**, *49*, 337–343. [CrossRef]
11.　Mourou, G.; Mironov, S.; Khazanov, E.; Sergeev, A. Single cycle thin film compressor opening the door to Zeptosecond-Exawatt physics. *Eur. Phys. J. Spec. Top.* **2014**, *223*, 1181–1188. [CrossRef]
12.　Ginzburg, V.N.; Yakovlev, I.V.; Zuev, A.S.; Korobeinikova, A.A.; Kochetkov, A.A.; Kuz'min, A.A.; Mironov, S.Y.; Shaykin, A.A.; Shaykin, I.A.; Khazanov, A.E. Compression after compressor: Threefold shortening of 200-TW laser pulses. *Quantum Electron.* **2019**, *49*, 299–301. [CrossRef]
13.　Balla, P.; Bin Wahid, A.; Sytcevich, I.; Guo, C.; Viotti, A.-L.; Silletti, L.; Cartella, A.; Alisauskas, S.; Tavakol, H.; Grosse-Wortmann, U.; et al. Postcompression of picosecond pulses into the few-cycle regime. *Opt. Lett.* **2020**, *45*, 2572–2575. [CrossRef] [PubMed]
14.　Ginzburg, V.; Yakovlev, I.; Zuev, A.; Korobeynikova, A.; Kochetkov, A.; Kuzmin, A.; Mironov, S.; Shaykin, A.; Shaikin, I.; Khazanov, E.; et al. Fivefold compression of 250-TW laser pulses. *Phys. Rev. A* **2020**, *101*, 013829. [CrossRef]

15. Ginzburg, V.N.; Yakovlev, I.V.; Zuev, A.S.; Korobeynikova, A.P.; Kochetkov, A.A.; Kuzmin, A.A.; Mironov, S.Y.; Shaykin, A.A.; Shaikin, I.A.; Khazanov, E.A. Two-stage nonlinear compression of high-power femtosecond laser pulses. *Quantum Electron.* **2020**, *50*, 331–334. [CrossRef]

16. Ginzburg, V.; Yakovlev, I.; Kochetkov, A.; Kuzmin, A.; Mironov, S.; Shaikin, I.; Shaykin, A.; Khazanov, E. 11 fs, 1.5 PW laser with nonlinear pulse compression. *Opt. Express* **2021**, *29*, 28297–28306. [CrossRef] [PubMed]

17. Khazanov, E.A.; Mironov, S.Y.; Mourou, G. Nonlinear compression of high-power laser pulses: Compression after compressor approach. *Phys.-Uspekhi* **2019**, *62*, 1096–1124. [CrossRef]

18. Anderson, D.P.; Lisak, M. Nonlinear asymmetric self-phase modulation and self-steepening of pulses in long optical waveguides. *Phys. Rev. A* **1983**, *27*, 1393–1398. [CrossRef]